Lithuanian Journal of Physics
Vol. **64**, No. 1, pp. 20–39 (2024)
ISSN 1648-8504 eISSN 2424-3647
DOI: https://doi.org/10.3952/physics.2024.64.1.3

SECOND-ORDER RAYLEIGH–SCHRÖDINGER PERTURBATION THEORY FOR THE GRASP2018 PACKAGE: CORE–VALENCE CORRELATIONS*

G. Gaigalas, P. Rynkun, and L. Kitovienė

Institute of Theoretical Physics and Astronomy, Vilnius University, Saulėtekio 3, 10257 Vilnius, Lithuania
Email: gediminas.gaigalas@tfai.vu.lt; pavel.rynkun@tfai.vu.lt; laima.radziute@tfai.vu.lt

Received 31 July 2023; accepted 4 August 2023

The General Relativistic Atomic Structure package [GRASP2018, C. Froese Fischer, G. Gaigalas, P. Jönsson, and J. Bieroń, Comput. Phys. Commun. (2019), DOI: 10.1016/j.cpc.2018.10.032] is based on multiconfiguration Dirac–Hartree–Fock and relativistic configuration interaction (RCI) methods for energy structure calculations. The atomic state function used in the program is built from the set of configuration state functions (CSFs). The valence–valence, core–valence and core–core correlations are explicitly included through expansions over CSFs in RCI. We present a combination of RCI and the stationary second-order Rayleigh–Schrödinger many-body perturbation theory in an irreducible tensorial form to account for electron core–valence correlations when an atom or ion has any number of valence electrons. This newly developed method, which offers two ways of use, allows a significant reduction of the CSF space for complex atoms and ions. We also demonstrate how the method and program works for the energy structure calculation of Cl III ion.

Keywords: configuration interaction, configuration state function generators, spin-angular integration, perturbation theory, tensorial algebra, core–valence correlations

PACS: 31.15.-p, 31.15.Ne, 31.30.Jv, 03.65.Pm

1. Introduction

There are many powerful theoretical methods for taking into account both relativistic and correlation effects in the calculation of atomic properties of any-electron atoms and ions in our days. This can be done, for example, by using various versions of the many-body perturbation theory (MBPT), the configuration interaction method (CI), the relativistic configuration interaction (RCI), the random phase approximation with exchange (RPAE), the multiconfiguration Hartree–Fock method (MCHF) [1] or the multiconfiguration Dirac–Hartree–Fock (MCDHF) method [2]. But each of them has its own disadvantages for getting atomic data in an extremely good accuracy. For example, converging to accurate results is very slow for MCHF, MCDHF and CI. This leads to a very large expansion of the atomic state function (ASF) for complex atoms. There are practical and theoretical difficulties with the perturbation theory for degenerate states, especially in the choice of model space [3]. The structure of terms of the perturbation theory (PT) series often leads to one- and two-particle operators which almost in all versions of many-body perturbation theory are not in an irreducible tensorial form and which cannot use the advantage of Racah algebra [4, 5].

The combination of CI and MBPT methods [6, 7] is probably the most efficient and consistent way to take into account simultaneously the correlation and relativistic effects in such complex many-electron atoms with open f-shells as lanthanides and actinides for calculations of energy spectra and other properties.

Here we present such an implementation of MBPT to the GRASP code [8] in which core–valence correlations can be taken into account with the help of MBPT and the rest of correlations are included in the ordinary way (RCI) by GRASP package. We use the most suitable for these systems irreducible

* Dedicated to the memory of professor **Adolfas Jucys** (1904–1974), pioneer of contemporary theoretical physics in Lithuania, initiator of the 'Lithuanian Physics Collection', on the occasion of his birth and death anniversaries.

tensorial form of Rayleigh–Schrödinger stationary many-body perturbation theory [9, 10]. This allows us to divide the calculation of terms of the perturbation series into the calculation of spin-angular terms by using Racah algebra [4, 5, 11] and into the accompanying radial integrals. The latter are more straightforward and can be handled by methods such as those of the GRASP code [8, 12]. Such packages have a modular structure, and modules for generating the contribution of diagrams representing terms of the MBPT series in an irreducible tensorial form can easily be added to the system. The newly developed method, which combines the RCI and the stationary second-order Rayleigh–Schrödinger many-body perturbation theory in an irreducible tensorial form (RCI+RSMBPT), and its implementation in the GRASP package is described in detail in the sections below.

2. General theory

2.1. Main theories in the GRASP package

The MCDHF method is based on the Dirac–Coulomb (DC) Hamiltonian [2, 13]

$$H_{\mathrm{DC}} = \sum_{i=1}^{N} (c\alpha_i \cdot \mathbf{p}_i + (\beta_i - 1)c^2 + V_i^N) + \sum_{i>j}^{N} \frac{1}{r_{ij}}, \quad (1)$$

where V^N is the monopole part of the electron–nucleus Coulomb interaction, α and β are the 4×4 Dirac matrices, and c is the speed of light in atomic units. The atomic state functions (ASFs) were obtained as linear combinations of symmetry adapted configuration state functions (CSFs) [14]

$$\Psi(\gamma PJM) = \sum_{j=1}^{N_{\mathrm{CSFs}}} c_j \cdot \Phi(\gamma_j PJM). \quad (2)$$

Here J and M are the angular quantum numbers, and P is parity. γ_j denotes other appropriate labelling of the configuration state function j, for example, the orbital occupancy and coupling scheme. Normally, the label γ of the atomic state function is the same as the label of the dominating CSF. For these calculations the spin-angular approach [4, 5], which is based on the second quantization in a coupled tensorial form, on the angular momentum theory in three spaces (orbital, spin and quasispin) and on the reduced coefficients of fractional parentage, was used. It allows us to study configurations with open f-shells without any restrictions. CSFs are built from products of one-electron Dirac orbitals. Based on a weighted energy average of several states, the so-called extended optimal level (EOL) scheme [15], both the radial parts of the Dirac orbitals and the expansion coefficients were optimized to self-consistency in the relativistic self-consistent field procedure [13].

In RCI computations, the atomic state function is expanded in CSFs, and only the expansion coefficients are determined by diagonalizing the Hamiltonian matrix [14]. The RCI method is also used to include the transverse-photon (Breit) interaction and QED corrections: vacuum polarization and self-energy [14]. More details about MCHDF and RCI methods can be found in Refs. [13, 14].

2.2. Zero-first-order method

One of Brillouin–Wigner perturbation theory versions is widely used by the GRASP community. In this version, according to the Brillouin–Wigner perturbation theory [3, 16], the CSF space can be divided into two parts:

(i) a principal part (P), which contains CSFs that account for the major parts of the wave functions and is referred to as zero-order partitioning;

(ii) an orthogonal complementary part (Q), which contains CSFs that represent minor corrections and is referred to as first-order partitioning.

The interaction between P and Q is assumed to be the lowest-order perturbation. The total energy functional is partitioned into the zero-order part ($H^{(0)}$) and the residual part (V). The Dirac–Fock energy functional is chosen as the zero-order part; the residual part then represents a correlation energy functional. The second-order Brillouin–Wigner perturbation theory then leads to

$$(E - H_{QQ}^{(0)})^{-1} V_{QP} \Psi_P = \Psi_Q,$$

$$[H_{PP}^{(0)} + V_{PP} + V_{PQ}(E - H_{QQ}^{(0)})^{-1} V_{QP}]\, \Psi_P = E\Psi_P. \quad (3)$$

The above equations define the first-order correlation operator and the second-order effective Hamiltonian operator for the P-space, respectively. In the brackets of the second equation, the first and the second terms compose the total energy functional in the P-space, and the third term represents the second-order correction to the correlation

energy functional in the *P*-space. The nonlinear effective Hamiltonian equation is written in a linearized form:

$$\begin{pmatrix} H_{PP}^{(0)} + V_{PP} & V_{PQ} \\ V_{QP} & H_{QQ}^{(0)} \end{pmatrix} \begin{pmatrix} \Psi_P \\ \Psi_Q \end{pmatrix} = E \begin{pmatrix} \Psi_P \\ \Psi_Q \end{pmatrix}. \quad (4)$$

The requirement that the total energy functional E is stationary with respect to variations in spin-orbitals ($\{\phi\}$) under the normalization and the orthogonality conditions leads to a set of the Euler–Lagrange equations

$$\frac{\delta E[\{\phi\}]}{\delta \phi_a} = \mu_a \phi_a + \sum_{b \neq a} \mu_{ab} \phi_b, \quad (5)$$

where $\{\mu\}$ are the Lagrange multipliers. The above equations are nothing but reduced MCDHF equations. That is to say, an apparent connection between the second-order Brillouin–Wigner perturbation energy functional and a set of reduced MCDHF equations is provided.

The block $H_{QQ}^{(0)}$ is diagonal in the Hamiltonian matrix (see Eq. (4)). As a result, the computation time and size required for the construction of the Hamiltonian matrix are reduced. This method, named as zero-first-order method (ZF), has the potential for taking a very large configuration space into account, which is almost unachievable by full MCDHF and RCI methods [14], and for allowing accurate calculation to be performed with relatively small computational resources, provided the *Q*-space contributes perturbatively to the *P*-space. However, all abovementioned methods (see Subsections 2.1 and 2.2) still lead to a very large space of ASF and need a big amount of computational resources in the case of very accurate calculations of complex atoms. So, the further improvements are welcome. One of the solutions to this problem is the implementation of the combination of RCI method with the Rayleigh–Schrödinger perturbation theory in an irreducible tensorial form in the Grasp using the usual PT formalism. This is discussed in the sections below.

2.3. Rayleigh–Schrödinger perturbation theory in irreducible tensorial form

The Brillouin–Wigner form of perturbation theory is formally very simple. However, the effective operator of second order depends on the exact energy of considered state. This requires a self-consistency procedure and limits the application to one energy level at a time. There are other issues with implementation of this theory [3] in the Grasp. The Rayleigh–Schrödinger perturbation theory, another version of PT, does not have these shortcomings, and therefore is more suitable for many-electron calculations than the Brillouin–Wigner PT.

There are several variations of the second-order Rayleigh–Schrödinger perturbation theory. Most of them deal with determinants instead of ASF in the form of Eq. (2). Only one of them [9, 10] is formulated in an irreducible tensorial form which gives the opportunity to include core–valence correlations with any number of valence electrons. This allows us to apply it to various applications using the combination [4] of the angular momentum theory [17], as described in Ref. [18], the concept of irreducible tensorial sets [19–21], a generalized graphical approach [22], the second quantization in a coupled tensorial form [21], the quasi-spin approach [23] and the use of reduced coefficients of fractional parentage [24], the same as used by the Grasp for calculation of one- and two-particle operators [11]. Given that the spin-angular structure of terms of the PT series of this version leads to one-, two- and three-particle operators in a tensorial form, this version [9, 10] of PT theory is ideal for the Grasp package.

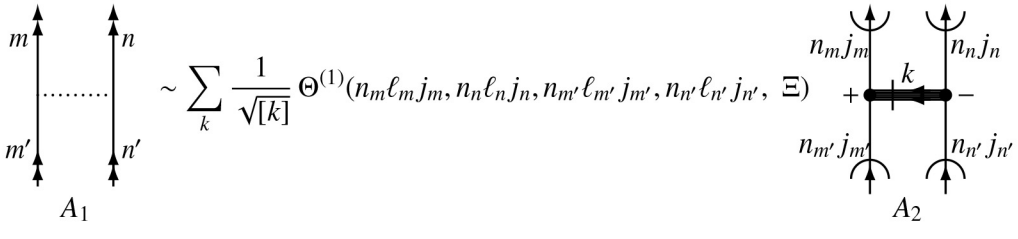

Fig. 1. Two-electron scalar operator when the second quantization operators are coupled by pairs $[a^{(j)} \times \tilde{a}^{(j')}]^{(k)}$.

The technique proposed in Ref. [9] leads to an effective Hamiltonian $\mathcal{H}_{\text{eff}}$ [25] in the second order PT, which can be expressed as the sum of terms corresponding to four classes of Feynman diagrams: vacuum, one-electron, two- electron and three-electron. We illustrate the construction by considering two Feynman diagrams: A_1 (Fig. 1) corresponds to a first-order two-electron diagram and A_3 (Fig. 2) corresponds to a second-order two-electron diagram. The following notation is used in these figures: $m \equiv n_m \ell_m j_m$, $m' \equiv n_{m'} \ell_{m'} j_{m'}$, $n \equiv n_n \ell_n j_n$, $n' \equiv n_{n'} \ell_{n'} j_{n'}$, $r \equiv n_r \ell_r j_r$, $s \equiv n_s \ell_s j_s$ and $a \equiv n_a \ell_a j_a$. The amplitude $\Theta^{(1)}(n_m \ell_m j_m, n_n \ell_n j_n, n_{m'} \ell_{m'} j_{m'}, n_{n'} \ell_{n'} j_{n'}, \Xi)$ is proportional to the two-electron one or two submatrix elements (the effective interaction strength) of a two-particle physical operator [4, 5, 10]

$$\Theta^{(1)}(n_m \ell_m j_m, n_n \ell_n j_n, n_{m'} \ell_{m'} j_{m'}, n_{n'} \ell_{n'} j_{n'}, \Xi) \sim$$

$$\sim \langle (n_m \ell_m) j_m (n_n \ell_n) j_n \| g_{12} \| (n_{m'} \ell_{m'}) j_{m'} (n_{n'} \ell_{n'}) j_{n'} \rangle \quad (6)$$

and

$$\Theta^{(2)}(n_m \ell_m j_m, n_n \ell_n j_n, n_{m'} \ell_m j_m, n_{n'} \ell_n j_n, n_r \ell_r j_r, n_s \ell_s j_s, \Xi) \sim$$

$$\sim \langle (n_m \ell_m) j_m (n_n \ell_n) j_n \| g_{12} \| (n_r \ell_r) j_r (n_s \ell_s) j_s \rangle \times$$

$$\times \langle (n_r \ell_r) j_r (n_s \ell_s) j_s \| g_{12} \| (n_{m'} \ell_{m'}) j_{m'} (n_{n'} \ell_{n'}) j_{n'} \rangle, \quad (7)$$

where Ξ is an array of intermediate coupling.

With the first Feynman diagram A_1, the GRASP package deals with the methods described in Sections 2.1 and 2.2. In Fig. 1, the left-hand side shows the interaction diagram and the dotted line corresponds to a two-electron interaction. This is decomposed into the product of reduced matrix elements composed of radial integrals and other algebraic expressions with a coupled tensor operator

$$A_2 := \left[\left[a^{(j_m)} \times \tilde{a}^{(j_{m'})} \right]^{(k)} \times \left[a^{(j_n)} \times \tilde{a}^{(j_{n'})} \right]^{(k)} \right]^{(0)}, \quad (8)$$

defined by the diagram A_2 in the right-hand side of Fig. 1. In Eq. (8), $a^{(j)}$ is an electron creation operator. Tensor $\tilde{a}^{(j)}$ is defined [21, 23] as

$$\tilde{a}^{(j)}_{m_j} = (-1)^{j-m_j} a^{\dagger(j)}_{-m_j}, \quad (9)$$

where $a^{\dagger(j)}_{-m_j}$ is an electron annihilation operator.

The second Feynman diagram A_3 is coming from the second order of perturbation theory and such type of diagrams (the second order of effective Hamiltonian) must be implemented in the GRASP. Similarly, the Feynman diagram A_3 is expressed as the product of a more complicated second-order perturbation expression with a recoupling coefficient A_4, and a coupled tensor operator A_5 with the same structure as A_2 (see Fig. 1). So, the diagrams are different, but the spin-angular part is the same: $A_2 = A_5$. Therefore this formulation of perturbation theory allows us to significantly simplify the calculation of an effective operator with any number of open subshells for complex atoms and ions by using the standard library of GRASP for spin-angular integration [11].

2.4. Relativistic second-order effective Hamiltonian of an atom or an ion in irreducible tensorial form

Originally, the irreducible tensorial form of Rayleigh–Schrödinger perturbation theory was formulated

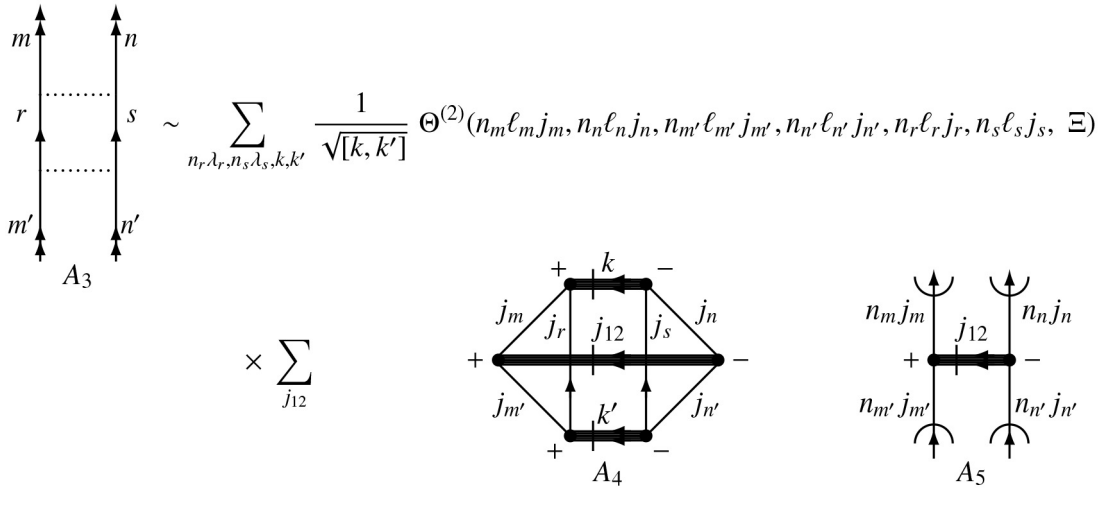

Fig. 2. One of the diagrams of the second-order effective Hamiltonian.

in nonrelativistic atomic theory that uses the *LS*-coupling [9, 10]. Here we derive from scratch such part of a second-order effective operator, which corresponds to core–valence (CV) correlations in relativistic atomic theory that uses the *jj*-coupling. For this we use the same technique as in Refs. [9, 10], that is, a generalized graphical approach [22] and the second quantization in a coupled tensorial form [21]. For this type of correlations we got two one-particle Feynman diagrams and four two-particle Feynman diagrams whose contribution to CV correlations is significant. These diagrams are expressed via scalar, multielectron operators which operate only in the space of the wave functions of open subshells and are not explicitly the functions of magnetic quantum numbers. Such form of an effective operator is very convenient in practical calculation of the energy spectra of atoms and ions with open electron subshells, because we can use all the advantages of methods described in Ref. [5]. For deriving the expression of an effective operator and applying it to calculation, the definition of module spaces must be determined. We use the same definitions in Refs. [3, 9, 10]. The effective operator itself is acting upon the *P*-space, similar as in the (i) paragraph of Subsection 2.2. The complementary part of the functional space is the orthogonal space or the *Q*-space, similar as in the (ii) paragraph of Subsection 2.2.

The module *P*-space, in addition to the *Q*-space, is normally broken down into three sets: -*F*, *F*′ and *G*. The *F* set includes the orbitals, which describe the filled (core) subshells encountered in all CSFs. Meanwhile the *F*′ set includes the orbitals, which correspond to the unfilled (valence) subshells in some of these CSFs or at least in one of them. The *G* set is built of the orbitals belonging to virtual subshells, which do not belong to *F* or *F*′ and are used for generating the CSF for counting correlation effects. To distinguish between these spaces in the Feynman diagrams and the algebraic notations, we use the following notations:

indexes *a* and *b* for the *F* set,

indexes *n*, *n*′, *m* and *m*′ for the *F*′ set,

indexes *r* and *s* for the *G* set.

In the following subsubsections, we will discuss in more detail each contribution of the Feynman diagram to core–valence correlations.

2.4.1. The first type of core–valence correlations

Here we will discuss the first type of core–valence correlations which are presented by one-particle Feynman diagrams in Figs. 3 and 4:

$$(n_a\ell_a)\, j_a^{2j_a+1}\, (n_{m'}\ell_{m'})\, j_{m'}^{w'_m} \;\rightarrow$$

$$\rightarrow\; (n_a\ell_a)\, j_a^{2j_a}\, (n_{m'}\ell_{m'})\, j_{m'}^{w'_m-1} (n_s\ell_s)\, j_s\, (n_r\ell_r)\, j_r. \qquad (10)$$

Each second-order Feynman diagram expression of perturbation theory has the energy denominator $D = \Sigma(\varepsilon_{\text{down}} - \varepsilon_{\text{up}})$, where $\varepsilon_{\text{down}}$ (ε_{up}) is the single-particle eigenvalue associated with the down-(up-) going orbital lines to (from) the lowest interaction line of diagram. For example, the denominator for CV_1 diagram in Fig. 3 is

$$D = (\varepsilon_{m'} + \varepsilon_a - \varepsilon_r - \varepsilon_s). \qquad (11)$$

The following notations are also used in the expressions of these diagrams (see Figs. 3 and 4):

$$X_k(ij, i'j') = \langle \ell_i j_i || C^{(k)} || \ell_{i'} j_{i'} \rangle \, \langle \ell_j j_j || C^{(k)} || \ell_{j'} j_{j'} \rangle \times$$

$$\times\, R^k(n_i j_i n_j j_j,\, n_{i'} j_{i'} n_{j'} j_{j'}). \qquad (12)$$

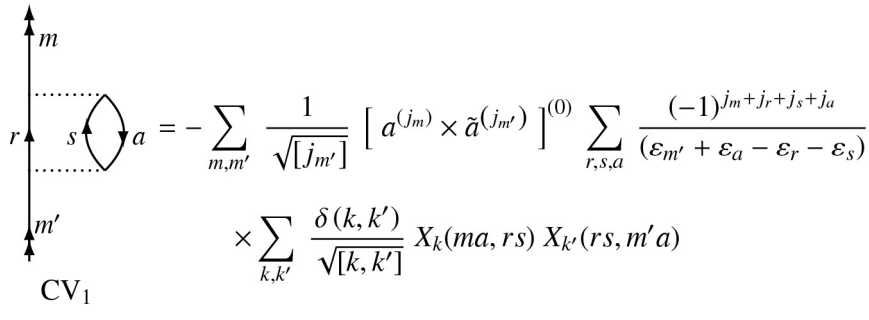

$$= -\sum_{m,m'} \frac{1}{\sqrt{[j_{m'}]}} \left[\, a^{(j_m)} \times \tilde{a}^{(j_{m'})} \,\right]^{(0)} \sum_{r,s,a} \frac{(-1)^{j_m+j_r+j_s+j_a}}{(\varepsilon_{m'} + \varepsilon_a - \varepsilon_r - \varepsilon_s)}$$

$$\times \sum_{k,k'} \frac{\delta(k,k')}{\sqrt{[k,k']}}\, X_k(ma, rs)\, X_{k'}(rs, m'a)$$

Fig. 3. The CV Feynman diagram of the second-order effective Hamiltonian for the direct part of excitation $(n_a\ell_a)\, j_a^{2j_a+1}\, (n_m\ell_{m'})\, j_{m'}^{w'_m} \rightarrow (n_a\ell_a)\, j_a^{2j_a}\, (n_{m'}\ell_{m'})\, j_{m'}^{w'_m-1} (n_s\ell_s)\, j_s\, (n_r\ell_r)\, j_r$.

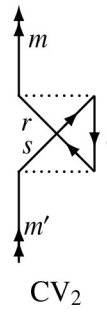

$$= -\sum_{m,m'} \frac{1}{\sqrt{[j_{m'}]}} \left[a^{(j_m)} \times \tilde{a}^{(j_{m'})} \right]^{(0)} \sum_{r,s,a} \frac{(-1)^{j_m+j_r+j_s+j_a}}{(\varepsilon_{m'} + \varepsilon_a - \varepsilon_r - \varepsilon_s)}$$

$$\times \sum_{k,k'} \begin{Bmatrix} k & j_m & j_r \\ k' & j_a & j_s \end{Bmatrix} X_k(ma, rs)\, X_{k'}(sr, m'a)$$

Fig. 4. The CV Feynman diagram of the second-order effective Hamiltonian for the exchange part of excitation $(n_a\ell_a)\, j_a^{2j_a+1}\, (n_{m'}\ell_{m'})\, j_{m'}^{w'_m} \rightarrow (n_a\ell_a)\, j_a^{2j_a}\, (n_{m'}\ell_{m'})\, j_{m'}^{w'_m-1}\, (n_s\ell_s)\, j_s\, (n_r\ell_r)\, j_r$.

Here $R^k\ (n_ij_in_jj_j,\ n_ij_{i'}n_jj_{j'})$ is the radial integral of the electrostatic interaction between electrons ([13], (89) and (90)), and $\langle \ell_i j_i || C^{(k)} || \ell_{i'} j_{i'} \rangle$ is the reduced matrix element of the irreducible tensor operator $C^{(k)}$ in the *jj*-coupling.

The spin-angular part of the diagrams CV_1 and CV_2 is the same, it has the normal order of creation and annihilation operators, it is in an irreducible tensorial form, and itself is a scalar operator

$$[a^{(j_m)} \times \tilde{a}^{(j_{m'})}]^{(0)}, \tag{13}$$

which acts only upon the F' set of P-space. The spin-angular part of these Feynman diagrams is the same as for the Dirac operator $\mathcal{H}_D$ [2, 13], with a reduced matrix element expressed through the spin-angular coefficient $t_{ab}^{\alpha\beta}$ and radial integrals $I(a, b)$ [11]. But the interaction strength is more complicated, having an additional coefficient such as 6*j*-symbol and an additional summation over the G set of orbitals. For example, the CV_2 diagram has

$$\frac{1}{\sqrt{[j_{m'}]}} \sum_{r,s,a} \frac{(-1)^{j_r+j_s-j_m-j_a}}{(\varepsilon_{m'} + \varepsilon_a - \varepsilon_r - \varepsilon_s)} \times$$

$$\times \sum_{k,k'} \begin{Bmatrix} k & j_m & j_r \\ k' & j_a & j_s \end{Bmatrix} X_k(ma, rs) X_{k'}(sr, m'a).$$

The same Feynman diagrams from Figs. 3 and 4 describe the core–valence correlations in the case $r \equiv s$ as well:

$$(n_a\ell_a)\, j_a^{2j_a+1}\, (n_{m'}\ell_{m'})\, j_{m'}^{w'_m} \rightarrow$$

$$\rightarrow (n_a\ell_a)\, j_a^{2j_a}\, (n_{m'}\ell_{m'})\, j_{m'}^{w'_m-1}\, (n_s\ell_s)\, j_s^2. \tag{14}$$

2.4.2. The second type of core–valence correlations

The second type of core–valence correlations

$$(n_a\ell_a)\, j_a^{2j_a+1}\, (n_{m'}\ell_{m'})\, j_{m'}^{w'_m}\, (n_{n'}\ell_{n'})\, j_{n'}^{w'_n} \rightarrow$$

$$\rightarrow (n_a\ell_a)\, j_a^{2j_a}\, (n_{m'}\ell_{m'})\, j_{m'}^{w'_m-1}\, (n_n\ell_{n'})\, j_{n'}^{w'_n+1} (n_r\ell_r)\, j_r \tag{15}$$

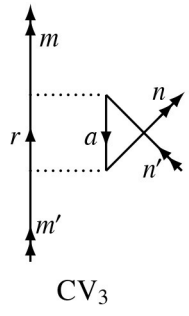

$$= \sum_{m,m'} \sum_{n,n'} \sum_{j_{12}} \sqrt{[j_{12}]} \left[\left[a^{(j_m)} \times \tilde{a}^{(j_{m'})} \right]^{(j_{12})} \times \left[\tilde{a}^{(j_{n'})} \times a^{(j_n)} \right]^{(j_{12})} \right]^{(0)}$$

$$\times \sum_{r,a} \sum_{k,k'} \frac{(-1)^{j_m+j_{m'}+k+k'}}{(\varepsilon_{m'} + \varepsilon_a - \varepsilon_r - \varepsilon_n)} \begin{Bmatrix} k & k' & j_{12} \\ j_{m'} & j_m & j_r \end{Bmatrix} \begin{Bmatrix} k & k' & j_{12} \\ j_n & j_{n'} & j_a \end{Bmatrix}$$

$$\times X_k(ma, rn')\, X_{k'}(rn, m'a)$$

Fig. 5. The CV Feynman diagram of the second-order effective Hamiltonian for the direct part of the second type of core–valence correlations $(n_a\ell_a)\, j_a^{2j_a+1}\, (n_{m'}\ell_{m'})\, j_{m'}^{w'_m} (n_{n'}\ell_{n'})\, j_{n'}^{w'_n} \rightarrow (n_a\ell_a)\, j_a^{2j_a}\, (n_{m'}\ell_{m'})\, j_{m'}^{w'_m-1}\, (n_n\ell_{n'})\, j_{n'}^{w'_n+1} (n_r\ell_r)\, j_r$.

can be expressed via one-particle (Figs. 3 and 4) and two-particle (Figs. 5, 6, 7, and 8) Feynman diagrams.

It is necessary to emphasize that the Feynman diagrams CV_3, CV_4, CV_5 and CV_6 are not in a normal order of creation and annihilation operators. The order of these operators in the tensorial product is the same as in Eq. (8) for CV_4, CV_5 and CV_6, while CV_3 is expressed via

$$\left[\left[a^{(j_m)}\times\tilde{a}^{(j_{m'})}\right]^{(j_{12})}\times\left[\tilde{a}^{(j_{n'})}\times a^{(j_n)}\right]^{(j_{12})}\right]^{(0)}. \quad (16)$$

All these operators in Eqs. (8) and (16) act only upon the F' set of P-space.

The spin-angular part of these Feynman diagrams is very similar as for the Coulomb operator [2, 13], which has been expressed in the normal order of second quantization operators as (see Eq. (20) in Ref. [4])

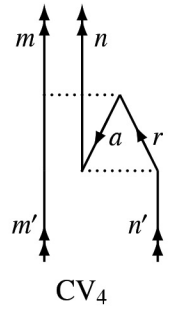

CV_4

$$= -\sum_{m,m'}\sum_{n,n'}\sum_{k}\frac{1}{\sqrt{[k]}}\left[\left[a^{(j_m)}\times\tilde{a}^{(j_{m'})}\right]^{(k)}\times\left[a^{(j_n)}\times\tilde{a}^{(j_{n'})}\right]^{(k)}\right]^{(0)}$$
$$\times\sum_{r,a}\sum_{k'}\frac{(-1)^{j_a+j_r+k}}{(\varepsilon_{n'}+\varepsilon_a-\varepsilon_r-\varepsilon_n)}\begin{Bmatrix}k & j_n & j_{n'}\\ k' & j_r & j_a\end{Bmatrix}X_k(ma,m'r)\,X_{k'}(nr,an')$$

Fig. 6. The CV Feynman diagram of the second-order effective Hamiltonian for the exchange part of the second type of core–valence correlations $(n_a\ell_a)\,j_a^{2j_a+1}\,(n_{m'}\ell_{m'})\,j_{m'}^{w'_m}(n_{n'}\ell_{n'})\,j_{n'}^{w'_n}\rightarrow(n_a\ell_a)\,j_a^{2j_a}\,(n_{m'}\ell_{m'})\,j_{m'}^{w'_m-1}(n_{n'}\ell_{n'})\,j_{n'}^{w'_n+1}(n_r\ell_r)\,j_r$.

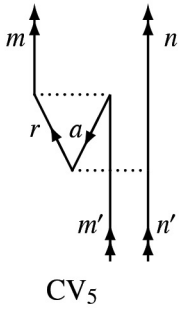

CV_5

$$= -\sum_{m,m'}\sum_{n,n'}\sum_{k'}\frac{1}{\sqrt{[k']}}\left[\left[a^{(j_m)}\times\tilde{a}^{(j_{m'})}\right]^{(k')}\times\left[a^{(j_n)}\times\tilde{a}^{(j_{n'})}\right]^{(k')}\right]^{(0)}$$
$$\times\sum_{r,a}\sum_{k}\frac{(-1)^{j_a+j_r+k'}}{(\varepsilon_{n'}+\varepsilon_a-\varepsilon_r-\varepsilon_n)}\begin{Bmatrix}k' & j_m & j_{m'}\\ k & j_a & j_r\end{Bmatrix}X_k(ma,rm')\,X_{k'}(rn,an')$$

Fig. 7. The CV Feynman diagram of the second-order effective Hamiltonian for the exchange part of the second type of core–valence correlations $(n_a\ell_a)\,j_a^{2j_a+1}\,(n_{m'}\ell_{m'})\,j_{m'}^{w'_m}(n_{n'}\ell_{n'})\,j_{n'}^{w'_n}\rightarrow(n_a\ell_a)\,j_a^{2j_a}\,(n_{m'}\ell_{m'})\,j_{m'}^{w'_m-1}(n_{n'}\ell_{n'})\,j_{n'}^{w'_n+1}(n_r\ell_r)\,j_r$.

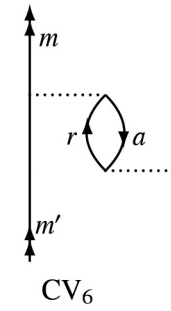

CV_6

$$= -\sum_{m,m'}\sum_{n,n'}\sum_{k,k'}\frac{\delta(k,k')}{[k]\sqrt{[k]}}\left[\left[a^{(j_m)}\times\tilde{a}^{(j_{m'})}\right]^{(k)}\times\left[a^{(j_n)}\times\tilde{a}^{(j_{n'})}\right]^{(k)}\right]^{(0)}$$
$$\times\sum_{r,a}\frac{(-1)^{j_a+j_r+k}}{(\varepsilon_{n'}+\varepsilon_a-\varepsilon_r-\varepsilon_n)}X_k(ma,m'r)\,X_{k'}(rn,an')$$

Fig. 8. The CV Feynman diagram of the second-order effective Hamiltonian for the exchange part of the second type of core–valence correlations $(n_a\ell_a)\,j_a^{2j_a+1}\,(n_{m'}\ell_{m'})\,j_{m'}^{w'_m}(n_{n'}\ell_{n'})\,j_{n'}^{w'_n}\rightarrow(n_a\ell_a)\,j_a^{2j_a}\,(n_{m'}\ell_{m'})\,j_{m'}^{w'_m-1}(n_{n'}\ell_{n'})\,j_{n'}^{w'_n+1}(n_r\ell_r)\,j_r$.

$$\left[\left[a^{(j_m)}\times a^{(j_n)}\right]^{(k)}\times\left[\tilde{a}^{(j_{m'})}\times\tilde{a}^{(j_{n'})}\right]^{(k)}\right]^{(0)}, \quad (17)$$

or in the combination of two parts in which the second quantization operators are ordered as pairs of creation-annihilation operators, like in Eqs. (8) and (13) (see Eq. (21) [4]).

Therefore, the program library [11] from Grasp supports the calculation of the spin-angular part of CV_4, CV_5 and CV_6 Feynman diagrams. In addition, it is very easy to redefine the expression (Eq. (16) to Eqs. (17) and (13)) of CV_3 diagram for the calculation of its spin-angular part with the program library [11].

2.4.3. The contribution of core–valence correlations to off-diagonal matrix elements

The main contribution of core–valence correlations to off-diagonal matrix elements is in the matrix element $\left\langle (n_m\ell_m)j_m^{w_m}(n_n\ell_n)j_n^{w_n}\,\|\,\hat{\mathcal{H}}^{(2)}_{\text{Effective}}\,\|\,(n_m\ell_m)j_m^{w_m-2}(n_n\ell_n)j_n^{w_n+2}\right\rangle$. The above contribution is derived from the excitation

$$(n_a\ell_a)j_a^{2j_a+1}(n_{m'}\ell_{m'})j_{m'}^{w'_m}(n_{n'}\ell_{n'})j_{n'}^{w'_n}\rightarrow$$
$$\rightarrow(n_a\ell_a)j_a^{2j_a}(n_{m'}\ell_{m'})j_{m'}^{w'_m-1}(n_{n'}\ell_{n'})j_{n'}^{w'_n+1}(n_r\ell_r)j_r, \quad (18)$$

and can be described by the same two-particle Feynman diagrams (Figs. 5, 6, 7 and 8) as before.

3. Implementation of Rayleigh–Schrödinger perturbation theory in irreducible tensorial form in the Grasp2018 [8]

The expressions of CV correlations in the second order of perturbation theory presented in Section 2.4 are exact and come directly from the theory. For the implementation of this theory in the RCI approach, we make the following assumptions:

1. Infinite summations over the *G* space are replaced by limited summations if our ASF in the zero order of perturbation theory is already sufficiently accurate. This is usually true after the RMCDHF calculation with the inclusion of valence–valence correlations or sometimes additionally CV excitation from one extreme trunk orbit. The correctness of this assumption is also confirmed by the accurate results obtained using the zero-first-order method in the Grasp package [27, 28], since this method is based on the Brillouin–Wigner perturbation theory, which is also subject to infinite summation, as is the case for the Rayleigh–Schrödinger perturbation theory.
2. In reality, the denominator of energy *D* (see Eq. (11)) in CV_1, CV_2, CV_3, CV_4, CV_5 and CV_6 contains only one-electron energies. But if in the combination of RCI and perturbation theory the one-electron orbitals are not spectroscopic (e.g. correlation orbitals [13, 26]), then the one-electron energies do not correspond to the values of the real one-electron energies and cannot be used in Eq. (11). Therefore in this case, we consider that the one-electron energies in the denominator *D* in CV_1, CV_2, CV_3, CV_4, CV_5 and CV_6 are changed to the averaged energies $\overline{D} = \overline{E}(K') - \overline{E}(K)$. $\overline{E}(K)$ is the averaged energy of a state for which calculations are performed. $\overline{E}(K')$ is the average energy for the admixed configuration *K′*. This allows us to move the energy denominator in front of summations over the orbitals belonging to the *F* and *G* set in the expressions of the second order of effective Hamiltonian [6, 29] and to simplify the implementation theory in the Grasp program package. It should be pointed out that *D* and $\overline{D}$ are defined differently in papers [9, 10] and [3,6, 29], respectively. In the first case, the energy of admixed configuration *K′* is with a minus sign in the energy difference *D*, while in the second case $\overline{D}$, on the contrary, it has the energy of the state under consideration *K*. We will also abide in the paper by these notations. Therefore, *D* and $\overline{D}$ will be defined with opposite signs.

For the calculation of average energies $\overline{E}(K)$ and $\overline{E}(K')$ we can use the analytical expression [11, (42)]

$$\bar{E} = \sum_a w_a I(a,a) +$$
$$+\sum_a \frac{w_a(w_a-1)}{2} \times \quad (19)$$
$$\times\left[F^0(a,a) - \frac{2j_a+1}{2j_a}\sum_{k>0}(\ell_a\ell_a k)\begin{pmatrix} j_a & k & j_a \\ -\frac{1}{2} & 0 & \frac{1}{2}\end{pmatrix}^2 F^k(a,a)\right] +$$
$$+\sum_{a<b} w_a w_b\left[F^0(a,b) - \sum_k(\ell_a\ell_b k)\begin{pmatrix} j_a & k & j_b \\ -\frac{1}{2} & 0 & \frac{1}{2}\end{pmatrix}^2 G^k(a,b)\right],$$

where symbol $(\ell_a\ell_b k)$ means that quantities ℓ_a, ℓ_b and k obey the triangular condition with

the even perimeter, which usually is included in the definition of radial integral [23, 11, 30].

A discussion on the correctness of these two assumptions is described in Subsection 4.1.

Brillouin–Wigner perturbation theory (with these assumptions) was already implemented in the GRASP package [8, 12] years ago. Accurate atomic data (with spectroscopic accuracy) [27, 31, 32] were obtained by using this method. Since such combination of the Brillouin–Wigner perturbation theory with the RCI method allows one to include correlation effects with a high accuracy, therefore the Rayleigh–Schrödinger perturbation theory (also other analogous perturbation theory option) combined with RCI and with the same assumption should also give accurate results. This can be confirmed by the investigation of energy spectra and transition data for a different ionization degree of a tungsten atom [34–36] or various other ions [37–39], including investigation of some metastable level along several isoelectronic sequences for the ions from $Z = 50$ to $Z = 92$ [40], and additionally calculating radiative lifetimes [41–43] by using a similar approach [6, 29] in the nonrelativistic atomic theory. Therefore, these two assumptions should not affect negatively the accuracy of CV correlations in the calculation of atomic properties with the combination of the CI approach with PT. But it is important that in the zero-order space the most important correlations would be included in this Rayleigh–Schrödinger perturbation theory [9, 10] and RCI combination, as it is done using RCI combined with Brillouin–Wigner perturbation theory.

It is more convenient to reformulate the formalism of perturbation theory presented in Subsection 2.3 in such a way that this would allow us to use the spin-angular library [11] without any modification and to make the easiest implementation of this theory in the GRASP2018 package [8] in general. This reformulation is presented here below.

According to Ref. [6], the contribution of the admixed configurations from CV correlations can be added to the usual energy of the term χJ of the configuration K (the set of $K\chi J$ and/or $K'\chi' J$ is the CSFs in the relativistic approach) and can be expressed as the energy E_0 (KJ), which does not depend on the term and the sum of the product of Slater integrals and spin-angular coefficients, describing the interaction within an open subshell and between them:

$$
\begin{aligned}
&E(K\chi J) = \\
&= E_0(KJ) + \Delta\varepsilon_0(KJ) + \\
&+\sum_{n\ell j}\sum_{k>0} \tilde{f}_k(\ell j^w, K\chi J)[\mathcal{F}^k(n\ell j, n\ell j) + \Delta\mathcal{F}^k(n\ell j, n\ell j)] + \\
&+\sum_{n\ell j}\sum_{n'\ell'j'>n\ell j}\left\{\sum_{k>0}\tilde{f}_k(\ell j^w \ell' j'^{w'}, K\chi J)\times\right. \\
&\qquad\times[\mathcal{F}^k(n\ell j, n'\ell' j') + \Delta\mathcal{F}^k(n\ell j, n'\ell' j')] + \\
&+\sum_{n\ell j}\tilde{g}_k(\ell j^w \ell' j'^{w'}, K\chi J)[\mathcal{G}^k(n\ell j, n'\ell' j') + \Delta\mathcal{G}^k(n\ell j, n'\ell' j')] + \\
&+\sum_{k}\tilde{v}_k(\ell j^w \ell' j'^{w'}, \ell j^{w-2}\ell' j'^{w'+2}, K\chi JK'\chi' J)\times \\
&\left.\times[\mathcal{R}^k(n\ell\, jn\ell j, n'\ell' j' n'\ell' j') + \Delta\mathcal{R}^k(n\ell jn\ell j, n'\ell' j' n'\ell' j')]\right\}, \qquad (20)
\end{aligned}
$$

where $\tilde{f}_k$, $\tilde{g}_k$ and $\tilde{v}_k$ are spin-angular coefficients from which submatrix elements $\langle \ell j||C^{(k)}||\ell' j'\rangle$ have been extracted. Therefore the summation over k runs over all possible values, instead of the values which satisfy the triangular condition ($\ell\ell' k$), as in the ordinary case of Eq. (19). The $\mathcal{F}^k(n\ell j,\ n'\ell' j')$, $\mathcal{G}^k(n\ell j,\ n'\ell' j')$ and $\mathcal{R}^k(n\ell jn\ell j,\ n'\ell' j'\ n'\ell' j')$ are generalized integrals of the electrostatic interaction between electrons. The definition of $\mathcal{R}^k(n\ell jn\ell j,\ n'\ell' j'\ n'\ell' j')$ is the following:

$$
\begin{aligned}
&\mathcal{R}^k(ij, i'j') = \\
&= \{[1+\delta(i,j)]\,[1+\delta(i',j')]\}^{-1/2} R^k(n_i j_i n_j j_j, n_i j_i n_{j'} j_{j'})\times \\
&\times \langle \ell_i j_i||C^{(k)}||\,\ell_i j_{i'}\rangle\langle \ell_j j_j||C^{(k)}||\ell_{j'} j_{j'}\rangle. \qquad (21)
\end{aligned}
$$

Here $R^k(n_i j_i n_j j_j,\ n_{i'} j_i n_{j'} j_{j'})$ is the same radial integral as in Eq. (12). Definitions $\mathcal{F}^k(n\ell j,\ n'\ell' j')$, $\mathcal{G}^k(n\ell j,\ n'\ell' j')$ follow straightforwardly from Eq. (21).

The contribution coming from the CV correlations of the configurations K' to $E(K\chi J)$ in the second order of perturbation theory can be written from Eq. (20) as

$$
\begin{aligned}
&\Delta E_{\mathrm{PT}} = \\
&=\Delta\mathcal{E}_0(KJ) + \\
&+\sum_{n\ell j}\sum_{k>0}\tilde{f}_k(\ell j^w, K\chi J)\,\Delta\mathcal{F}^k(n\ell j, n\ell j) + \\
&+\sum_{n\ell j}\sum_{n'\ell' j'>n\ell j}\left\{\sum_{k>0}\tilde{f}_k(\ell\, j^w\, \ell' j'^{w'}, K\chi J)\Delta\mathcal{F}^k(n\ell j, n'\ell' j') + \right. \\
&+\sum_{n\ell j}\tilde{g}_k(\ell j^w \ell' j'^{w'}, K\chi J)\ \Delta\mathcal{G}^k(n\ell j,\ n'\ell' j') + \\
&+\sum_{k}\tilde{v}_k(\ell j^w \ell' j'^{w'}, \ell j^{w-2}\ell' j'^{w'+2}, K\chi J\, K'\chi' J)\times \\
&\left.\times\Delta\mathcal{R}^k(n\ell jn\ell j, n'\ell' j' n'\ell' j')\right\}. \qquad (22)
\end{aligned}
$$

Table 1. Expressions for core–valence corrections to the energy in Eq. (20), not depending on the term.

$\Delta\mathcal{E}_0$ corrections
$\overbrace{(n_a\ell_a)j_a^{2j_a+1}}^{\text{core subshells}}\overbrace{(n_m\ell_m)j_m^{w_m}}^{\text{valence subshells}}\rightarrow\overbrace{(n_a\ell_a)j_a^{2j_a}}^{\text{core subshells}}\overbrace{(n_m\ell_m)j_m^{w_m-1}}^{\text{valence subshells}}\overbrace{(n_s\ell_s)j_s(n_r\ell_r)j_r}^{\text{virtual subshells}}$ $-\frac{w_m}{[j_m]}\left\{\underbrace{2(-1)^{j_r+j_s+j_m+j_a}\sum_k\mathcal{C}\ (k,ma,rs)}_{\text{from CV}_2\text{ Feynman diagram}}+\underbrace{\sqrt{[j_m]}\left[\sqrt{[j_r]}\mathcal{A}(0,ma,sr)+\sqrt{[j_s]}\mathcal{A}(0,ma,rs)\right]}_{\text{from CV}_1\text{ Feynman diagram}}\right\}$
$\overbrace{(n_a\ell_a)j_a^{2j_a+1}}^{\text{core subshells}}\overbrace{(n_m\ell_m)j_m^{w_m}}^{\text{valence subshells}}\rightarrow\overbrace{(n_a\ell_a)j_a^{2j_a}}^{\text{core subshells}}\overbrace{(n_m\ell_m)j_m^{w_m-1}}^{\text{valence subshells}}\overbrace{(n_s\ell_s)j_s^2}^{\text{virtual subshells}}$ $\frac{2w_m}{[j_m]}\left\{\underbrace{(-1)^{j_m+j_a}\sum_k\mathcal{C}\,(k,ma,ss)}_{\text{from CV}_2\text{ Feynman diagram}}\underbrace{-\sqrt{[j_m,j_s]}\mathcal{A}(0,ma,ss)}_{\text{from CV}_1\text{ Feynman diagram}}\right\}$
$\overbrace{(n_a\ell_a)j_a^{2j_a+1}}^{\text{core subshells}}\overbrace{(n_m\ell_m)j_m^{w_m}(n_n\ell_n)j_n^{w_n}}^{\text{valence subshells}}\rightarrow\overbrace{(n_a\ell_a)j_a^{2j_a}}^{\text{core subshells}}\overbrace{(n_m\ell_m)j_m^{w_m-1}(n_n\ell_n)j_n^{w_n+1}}^{\text{valence subshells}}\overbrace{(n_r\ell_r)j_r}^{\text{virtual subshells}}$ $\underbrace{-\frac{w_m([j_n]-w_n)}{\sqrt{[j_m,j_n]}}\mathcal{A}(0,ma,rn)}_{\text{from CV}_3\text{ Feynman diagram}}-\frac{(-1)^{j_m+j_n+j_r+j_a}w_m}{[j_m]}\left\{\underbrace{2\sum_k\mathcal{C}\,(k,ma,nr)}_{\text{from CV}_2^r\text{ and CV}_2^s\text{ Feynman diagrams}}\ \underbrace{+\sum_k\frac{1}{[k]}\mathcal{P}(kk,ma,nr)}_{\text{from CV}_1^s\text{ Feynman diagram}}\right\}$

The first type contribution of CV correlations in the second order of perturbation theory is expressed only over $\Delta\mathcal{E}_0(KJ)$ (see Table 1). The contributions $\Delta\mathcal{F}^k(n\ell j, n\ell j)$, $\Delta\mathcal{F}^k(n\ell j, n'\ell'j')$ and $\Delta\mathcal{G}^k(n\ell j, n'\ell'j')$ are equal to zero in this case. The contributions $\Delta\mathcal{E}_0(KJ)$ can be expressed through $\mathcal{A}$ and $\mathcal{C}$ coefficients (see Table 1) which have the following expressions:

$$\mathcal{A}(x,ij,i'j') = \\ = \sum_{k,k'}\begin{Bmatrix} k & k' & x \\ j_i & j_i & j_{i'}\end{Bmatrix}\begin{Bmatrix} k & k' & x \\ j_{j'} & j_{j'} & j_j\end{Bmatrix}\mathcal{P}(kk',ij,i'j'), \quad (23)$$

$$\mathcal{C}(k,ij,i'j') = \sum_{k'}\begin{Bmatrix} k & j_i & j_{i'} \\ k' & j_j & j_{j'}\end{Bmatrix}Q(kk',ij,i'j'), \quad (24)$$

where

$$\mathcal{P}(kk',ij,i'j') = \mathcal{R}^k(ij,i'j')\,\mathcal{R}^{k'}(i'j',ij)\,\mathcal{O}(K',K), \quad (25)$$

$$Q(kk',ij,i'j') = \mathcal{R}^k(ij,i'j')\,\mathcal{R}^{k'}(i'j',ji)\,\mathcal{O}(K',K). \quad (26)$$

We would like to emphasize once more that the energy denominator is defined differently/opposite in the expressions of Feynman diagrams (see, for example, Fig. 3, Eqs. (25) and (26)):

$$\mathcal{O}(K',K) = \frac{1}{\bar{E}(K') - \bar{E}(K)}. \quad (27)$$

The second type contribution of CV correlations in the second order of perturbation theory is expressed over $\Delta\mathcal{E}_0(KJ)$, $\Delta\mathcal{F}^k(n\ell j, n\ell j)$, $\Delta\mathcal{F}^k(n\ell j, n'\ell'j')$ and $\Delta\mathcal{G}^k(n\ell j, n'\ell'j')$ (see Tables 1 and 2).

The Feynman diagram with the notation CV_1^s in Table 2 means the same Feynman diagram CV_1 (see Fig. 3), but instead of the index s belonging to the G type of orbitals the index n which belongs to the F' type of orbitals is used. Similarly, in the Feynman diagrams with the notations CV_2^r and CV_2^s (Table 2), the index r (index s) is changed to the index n (index n). These types of the Feynman diagrams come from the reordering the operators of second quantization from the coupled by pairs $[a^{(j)}\times\tilde{a}^{(j')}]^{(k)}$

Table 2. Expressions for the Slater integrals $\Delta\mathcal{F}^k(m, n)$ and $\Delta\mathcal{G}^k(m, n)$ (see Eq. (20)) corresponding to the second type of core–valence $(n_a\ell_a)\, j_a^{2j_a+1}\, (n_{m'}\ell_{m'})\, j_{m'}^{w'_m}\, (n_n\ell_{n'})\, j_{n'}^{w'_n} \rightarrow (n_a\ell_a)\, j_a^{2j_a}\, (n_{m'}\ell_{m'})\, j_{m'}^{w'_m-1}\, (n_n\ell_{n'})\, j_{n'}^{w'_n+1}\, (n_r\ell_r)\, j_r$ correlations.

Corrections	Slater integral	k values
$\underbrace{[k]\mathcal{Y}(1,k,ma,rn,mn)}_{\text{from CV}_3\text{ Feynman diagram}}$	$\Delta\mathcal{F}^k(m, n)$	$k > 0$
$\underbrace{2\,(-1)^{j_r+j_a+k}\,\mathcal{Z}\,(1,k,ma,nr,mn)}_{\text{from CV}_4\text{ and CV}_5\text{ Feynman diagrams}} + \underbrace{\frac{(-1)^{j_r+j_a+k}}{[k]}\mathcal{P}\,(kk,ma,nr)}_{\text{from CV}_6\text{ Feynman diagram}}$	$\Delta\mathcal{G}^k(m, n)$	$k \geq 0$

order to the normal order of operators of second quantization. The diagram CV_1^s comes after the reorder of the diagram CV_6, the diagram CV_2^r comes after the reorder of the diagram CV_4, and the CV_2^s comes after the reorder of the diagram CV_5. This reordering allows us to have the same spin-angular part of the diagrams CV_4, CV_5 and CV_6 as any two-particle operator in the GRASP:

$$\mathcal{Y}(I,x,ij,i'j',i''j'') = \\ = \sum_{k,k'}(-1)^{k+k'+x}\begin{Bmatrix} k & k' & x \\ j_{i''} & j_i & j_{i'} \end{Bmatrix}\begin{Bmatrix} k & k' & x \\ j_{j''} & j_{j'} & j_j \end{Bmatrix}\mathcal{T}(I,kk',ij,i'j',i''j''), \tag{28}$$

$$\mathcal{T}(I,kk',ij,i'j',i''j'') = \\ = \begin{cases} \mathcal{R}^k(ij,i'j')\mathcal{R}^{k'}(i'j'',i''j)\mathcal{O}(K',K) & \text{for } I=1, \\ \mathcal{R}^k(ij,i'j')\mathcal{R}^{k'}(i'j'',i''j)\,\mathcal{O}(K',K_1K_2) & \text{for } I=2, \end{cases} \tag{29}$$

where

$$\mathcal{O}(K',K_1K_2) = \\ = \frac{1}{2}\left(\frac{1}{\bar{E}(K') - \bar{E}(K_1)} + \frac{1}{\bar{E}(K') - \bar{E}(K_2)}\right). \tag{30}$$

$$\mathcal{Z}(I,k,ij,i'j',i''j'') = \\ = \sum_{k'}\begin{Bmatrix} k & j_{i''} & j_{j''} \\ k' & j_j & j_{j'} \end{Bmatrix}\mathcal{U}(I,kk',ij,i'j',i''j''), \tag{31}$$

$$\mathcal{U}(I,kk',ij,i'j',i''j'') = \\ = \begin{cases} \mathcal{R}^k(ij,i'j')\mathcal{R}^{k'}(j''j', ji'')\mathcal{O}(K',K) & \text{for } I=1, \\ \mathcal{R}^k(i'j',ij)\mathcal{R}^{k'}(i''j, j'j'')\mathcal{O}(K',K) & \text{for } I=2, \\ \mathcal{R}^k(ij,i'j')\mathcal{R}^{k'}(j''j', ji'')\mathcal{O}(K',K_1K_2) & \text{for } I=3, \\ \mathcal{R}^k(i'j',ij)\mathcal{R}^{k'}(i''j, j'j'')\mathcal{O}(K',K_1K_2) & \text{for } I=4. \end{cases} \tag{32}$$

There are the following symmetries for $\mathcal{Z}$ coefficients:

$$\mathcal{Z}\,(1, k, ij, i'j'\, ii') = \mathcal{Z}(2, k, ij, i'j'\, ii'), \tag{33}$$

$$\mathcal{Z}\,(3, k, ij, i'j'\, i'i) = \mathcal{Z}(4, k, ij, i'j'\, i'i). \tag{34}$$

The contribution of CV correlation in the second order of perturbation theory coming from the off-diagonal matrix element $\left\langle (n_m\ell_m)\, j_m^{w_m}\, (n_n\ell_n)\, j_n^{w_n} \,\|\, \hat{\mathcal{H}}^{(2)}_{\text{Effective}} \,\|\, (n_m\ell_m)\, j_m^{w_m-2}\, (n_n\ell_n)\, j_n^{w_n+2} \right\rangle$ is described by the diagrams CV_3, CV_4, CV_5 and CV_6. The reformulation expressions of these diagrams to the form suitable to the GRASP gave these corrections only to the radial integral $\Delta\mathcal{R}^k(mm, nn)$ (see Table 3). All these formulas are expressed via the quantities introduced earlier in the paper, except

$$\mathcal{S}(kk', ij, i'j', i''j'') = \\ = \mathcal{R}^k\,(ij, i'j')\,\mathcal{R}^{k'}\,(j'i'', jj'')\,\mathcal{O}(K', K_1K_2). \tag{35}$$

This theory in an irreducible tensorial form is more suitable to be included in such a version of the GRASP that is based on the configuration of state function generators (CSFGs) [33]. This is related to the fact that this version of the package allows us to distinguish the *F*, *F*′ and *G* sets of orbitals very easily in the process of computing atomic data. In the following section, we will present a test case of this implementation.

4. Calculation of core–valence correlations with new implementation

This section is intended to present the results using here the newly developed and presented method, based on the Rayleigh–Schrödinger perturbation theory in an irreducible tensorial form, which is implemented in the GRASP2018 package.

Table 3. Expressions for the Slater integral $\Delta\mathcal{R}^k(mm, nn)$ (see Eq. (20)) corresponding to the core–valence $(n_a\ell_a)\, j_a^{2j_a+1}\,(n_{m'}\ell_{m'})\, j_{m'}^{w'_m}\,(n_{n'}\ell_{n'})\, j_{n'}^{w'_n} \rightarrow (n_a\ell_a)\, j_a^{2j_a}\,(n_{m'}\ell_{m'})\, j_{m'}^{w'_m-1}\,(n_{n'}\ell_{n'})\, j_{n'}^{w'_n+1}\,(n_r\ell_r)\, j_r$ correlations coming from the off-diagonal matrix element $\left\langle (n_m\ell_m)\, j_m^{w_m}\,(n_n\ell_n)\, j_n^{w_n} \,\|\, \hat{\mathcal{H}}^{(2)}_{\text{Effective}} \,\|\, (n_m\ell_m) j_m^{w_m-2}\,(n_n\ell_n)\, j_n^{w_n+2} \right\rangle$.

Corrections	Slater integral	k values
$2\Big\{\underbrace{[k]\,\mathcal{Y}(2,k,ma,rn,nm)}_{\text{from CV}_3\text{ Feynman diagram}} + \underbrace{+(-1)^{j_r+j_a+k}\,\mathcal{Z}(3,k,ma,nr,nm)}_{\text{from CV}_4\text{ Feynman diagram}} + \underbrace{(-1)^{j_r+j_a+k}\,\mathcal{Z}(4,k,na,mr,mn)}_{\text{from CV}_5\text{ Feynman diagram}} + \underbrace{+\frac{(-1)^{j_r+j_a+k}}{[k]}\,\mathcal{S}(kk,ma,nr,mn)}_{\text{from CV}_6\text{ Feynman diagram}}\Big\}$	$\Delta\mathcal{R}^k(mm, nn)$	$k \geq 0$

This new developed method allows us to include the CV correlations in the computations choosing the preferred core and virtual orbitals. Using this method we can open the core fully and estimate the impact of CV correlations in the second order of perturbation theory for the computed levels. To calculate the contributions of such CV correlations the average energies of the configurations are needed. There are three options to calculate the average energy of configuration in the program implemented in the GRASP2018 package:

- The average energy is calculated using an analytical expression (Eq. (19)) (option 0);
- The average energy is calculated according to the diagonal matrix element (option 1);
- The average energy is calculated by discarding those energies for which the non-diagonal matrix elements with the multi-reference set are zero (option 2).

The results from the computations using the new method will be marked as CV RCI+RSMBPT (according to Eq. (20)). To evaluate the accuracy and the reliability of the results, these are compared with the results from the rearranged RCI method, based on CSFGs [33], which compute only the CV correlations (results marked as CV RCI).

4.1. The first test case

In the first test, 3 energy levels of the ground ($1s^22s^22p^63s^23p^3$) configuration with J = 3/2 of the Cl III ion are computed. The multi-reference (MR) set consists of 3 CSFs ($3s^23p^3$, $3s^23p\_3p^2$ and $3s^23p^2\_3p$ in *jj*-coupling) belonging to the $3s^23p^3$ configuration from which substitutions are allowed to include CV correlations. The 1s, 2s, 2p_ and 2p subshells are defined as opened core subshells (F set), 3s, 3p_ and 3p as valence subshells (F' set), and 4s, 4p_, 4p, 3d_ and 3d as virtual ones (G set). Such set of virtual orbitals will be marked as L1. So the CSFs list consists of 3 CSFs belonging to the MR set, and the rest CSFs are the CV correlations of the MR set. Radial wave functions are taken from the earlier computations [44].

Firstly, we will check the expressions derived in Subsections 2.4 and 3. As described in Section 3, several types of CV correlations are implemented. Here below, the contributions for each type of the CV correlations will be compared with the results from CV RCI computations. To calculate the contribution of a particular K' configuration of the CV correlations from the RCI, based on the CSFGs, for the first and second type (see Tables 1 and 2) we will use the equation

$$\Delta E_{\text{PT}} = -\frac{\Sigma_{\chi'}\,|\langle (K\chi J)\,\|\,V\,\|\,(K'\chi' J)\rangle\,|^2}{\bar{E}(K') - \bar{E}(K)} \qquad (36)$$

and

$$\Delta E_{\text{PT}} = -\frac{\Sigma_{\chi'}\langle (K_1\chi J)\,\|\,V\,\|\,(K'\chi' J)\rangle\langle (K_2\chi J)\,\|\,V\,\|\,(K'\chi' J)\rangle}{2} \times \times\left(\frac{1}{\bar{E}(K') - \bar{E}(K_1)} + \frac{1}{\bar{E}(K') - \bar{E}(K_2)}\right), \qquad (37)$$

to compute the effect from off-diagonal matrix elements (see Table 3).

The results of these examples for the first and second types of CV correlations are presented in Table 4. Matrix elements and average energies (with option 0) are given there. The CV contribution from CV RCI+RSMBPT computations is compared with the contribution calculated by Eq. (36). As seen from Table 4, there is an excellent agreement between two computations. For the first type the effect of CV correlations is –2.48300702640003E-04 a.u. by Eq. (36) and –2.48300702643986E-04 a.u. by Eq. (22); for the second type of CV correlations it is –5.30286558582154E-05 a.u. by Eq. (36) and –5.30286558628605E-05 a.u. by Eq. (22). The example for the contribution of CV correlations to off-diagonal matrix elements is presented in Table 5. It is seen that there is an excellent agreement between both calculations (7.74908996437684E-06 a.u. by Eq. (37) and 7.74908996512910E-06 a.u. by Eq. (22)). By using the Rayleigh–Schrödinger perturbation theory in an irreducible tensorial form to calculate the contribution of CV correlations 14 numbers after comma are reproduced.

The energy structure results from both (CV RCI and CV RCI +RSMBPT) computations are given in Table 6. For the CV RCI case in the RCI computations the ZF method is also applied. The MR space is used as the principal part *P*. In the CV RCI+RSMBPT case, the results from three computations (different options of averaging energies) are presented. As seen from Table 6, the differences between the CV RCI and CV RCI+RSMBPT (option 0) calculations are 0.0000489 a.u., 0.0000519 a.u. and 0.0000568 a.u., whereas the contributions of CV correlations are –0.0022369 a.u., –0.0022419 a.u. and –0.0022510 a.u., respectively, for the $^4S_{3/2}$, $^2D_{3/2}$ and $^2P_{3/2}$ levels. The disagreement between the results in this case is only 2.2–2.5%. This disagreement decreases when in the CV RCI+RSMBPT computations the energy of configuration is averaged according to the diagonal matrix element (option 1), to 1.4–2.0%. There is

Table 4. Comparison of the contribution of the first and second type of CV correlations from the CV RCI and CV RCI+RSMBPT computations. The contribution of K' CV correlations is given for the computed level $1s^22s^22p^_2p^43s^23p^3$.

$K'\chi'J = 3/2$	$\langle(K\chi J = 3/2)\|\|V\|\|(K'\chi'J = 3/2)\rangle$	Energy, a.u.
$1s^22s^22p^_2p^43s^23p^23d^_3d$ (the first type of CV, see Subsection 2.4.1)		
$1s^22s^22p^_2p^43s^23p^2(0)3d^_ < 1 > 3d$	1.9323531771818409E-02	$\bar{E}\,(K) = -459.55556158934053$
$1s^22s^22p^_2p^43s^23p^2(0)3d^_ < 2 > 3d$	1.1447066004165937E-03	$\bar{E}\,(K') = -450.50099438062546$
$1s^22s^22p^_2p^43s^23p^2(2) < 3/2 > 3d^_ < 1 > 3d$	–1.0237704805308916E-03	
$1s^22s^22p^_2p^43s^23p^2(2) < 3/2 > 3d^_ < 2 > 3d$	1.0152134678921704E-02	
$1s^22s^22p^_2p^43s^23p^2(2) < 3/2 > 3d^_ < 3 > 3d$	–2.8273270317335265E-02	
$1s^22s^22p^_2p^43s^23p^2(2) < 5/2 > 3d^_ < 1 > 3d$	–6.0999204304291775E-03	
$1s^22s^22p^_2p^43s^23p^2(2) < 5/2 > 3d^_ < 2 > 3d$	1.8300440014309707E-02	
$1s^22s^22p^_2p^43s^23p^2(2) < 5/2 > 3d^_ < 3 > 3d$	–2.4406821873536943E-02	
$1s^22s^22p^_2p^43s^23p^2(2) < 5/2 > 3d^_ < 4 > 3d$	–1.4987727556927458E-03	
ΔE_{PT} = –2.48300702640003E-04 a.u. (by Eq. (36))		
ΔE_{PT} = –2.48300702643986E-04 a.u. (by Eq. (22))		
$1s^22s^22p^_2p^43s3p^_3p^34s$ (the second type of CV, see Subsection 2.4.2)		
$1s^22s^22p^_2p^43s < 0 > 3p^_ < 1/2 > 3p^3 < 1 > 4s$	7.9640894479663035E-03	$\bar{E}\,(K) = -459.55556158934053$
$1s^22s^22p^_2p^43s < 0 > 3p^_ < 1/2 > 3p^3 < 2 > 4s$	1.0281595266559909E-02	$\bar{E}\,(K') = -450.58662000712661$
$1s^22s^22p^_2p^43s < 1 > 3p^_ < 1/2 > 3p^3 < 1 > 4s$	1.0720418507720091E-02	
$1s^22s^22p^_2p^43s < 1 > 3p^_ < 1/2 > 3p^3 < 2 > 4s$	1.3840000781591226E-02	
$1s^22s^22p^_2p^43s < 1 > 3p^_ < 3/2 > 3p^3 < 1 > 4s$	0.0	
$1s^22s^22p^_2p^43s < 1 > 3p^_ < 3/2 > 3p^3 < 2 > 4s$	0.0	
ΔE_{PT} = –5.30286558582154E-05 a.u. (by Eq. (36))		
ΔE_{PT} = –5.30286558628605E-05 a.u. (by Eq. (22))		

Table 5. Comparison of the contribution of CV correlations to the off-diagonal matrix elements from the CV RCI and CV RCI+RSMBPT computations. The contribution of K' CV correlations is given to the off-diagonal matrix elements between the computed levels $1s^22s^22p^-_22p^4_-3s^23p^3$ (K_1) and $1s^22s^22p^-_22p^4_-3s^23p^-_23p$ (K_2).

$K'\chi'J = 3/2$	$\langle(K_1\chi J = 3/2)\|\|V\|\|(K'\chi'J = 3/2)\rangle$	$\langle(K_2\chi J = 3/2)\|\|V\|\|(K'\chi'J = 3/2)\rangle$
$1s^22s2p^-_22p^4_-3s^23p_-3p^23d$ (off-diagonal, see Subsection 2.4.3)		
$1s^22s2p^-_22p^4_-3s^23p_- < 1 > 3p^2(0)3d$	2.5856710447641450E-03	8.0873774303662094E-03
$1s^22s2p^-_22p^4_-3s^23p_- < 0 > 3p^2(2) < 2 > 3d$	0.0	0.0
$1s^22s2p^-_22p^4_-3s^23p_- < 1 > 3p^2(2) < 1 > 3d$	–8.1766097814018907E-04	2.5574532977397013E-03
$1s^22s2p^-_22p^4_-3s^23p_- < 1 > 3p^2(2) < 2 > 3d$	–2.7928439287496273E-03	8.7353660093932462E-03
$1s^22s2p^-_22p^4_-3s^23p_- < 1 > 3p^2(2) < 3 > 3d$	–4.9959911001853999E-03	1.5626297764275494E-02
$\bar{E}$ (K_1) = –459.55556158934053 a.u.		
$\bar{E}$ (K_2) = –459.56656073844789 a.u.		
$\bar{E}$ (K') = –448.76686304559024 a.u.		
ΔE_{PT} = 7.74908996437684E-06 a.u. (by Eq. (37))		
ΔE_{PT} = 7.74908996512910E-06 a.u. (by Eq. (22))		

a little decrease when average energy is calculated by discarding those energies for which the non-diagonal matrix elements with the multi-reference set are zero (option 2). Comparing the CV RCI+RSMBPT with the results from CV RCI ZF, this disagreement decreases to 0.1–0.7% in option 2. We want to note that the difference between the CV RCI and CV RCI+RSMBPT computations for 3 computed levels is similar and stable (about 0.00005 a.u with option (0)). Meanwhile comparing the CV RCI+RSMBPT results with the results from CV RCI ZF these differences differ for each computed level and are 0.0000343 a.u., 0.0000144 a.u. and 0.0000007 a.u., respectively, for the first, the second and the third level. Comparing the splitting of the computed levels from CV RCI and CV RCI +RSMBPT computations, we see that splitting from CV RCI+RSMBPT is closer to the CV RCI results than CV RCI ZF.

The obtained results and comparisons made lead us to the following that the expressions of Rayleigh–Schrödinger perturbation theory in an irreducible tensorial form derived in Subsections 2.4 and 3 are correct, the assumptions made in Section 3 are not materially wrong, and the program based on this methodology is free from bugs. Thus it means that the direct inclusion of correlations with the Brillouin–Wigner perturbation theory from Subsection 2.2 can be substituted for by the version of the Rayleigh–Schrödinger perturbation theory presented in Subsection 2.4. It is appropriate because by using the combination of the RCI and the Rayleigh–Schrödinger perturbation theory in an

Table 6. The energy levels (in cm^{-1}) and total energies (in a.u.) for 3 energy levels of the $3s^23p^3$ configuration with J = 3/2 are given from both computations when CV correlations are included. 0, 1 and 2 columns mark the options of averaging the energy of the configuration.

No.	State	MR	CV RCI		CV RCI+RSMBPT		
				ZF	0	1	2
			Energy levels (cm^{-1})				
1	$3s^23p^3\ ^4S_{3/2}$	0.00	0.00	0.00	0.00	0.00	0.00
2	$3s^23p^3\ ^2D_{3/2}$	23142.25	23141.15	23136.12	23140.51	23140.23	23140.32
3	$3s^23p^3\ ^2P_{3/2}$	38735.68	38732.59	38723.48	38730.87	38729.48	38729.83
			Total energy (a.u.)				
1	$3s^23p^3\ ^4S_{3/2}$	–459.6785245	–459.6807614	–459.6807760	–459.6808103	–459.6807921	–459.6807918
2	$3s^23p^3\ ^2D_{3/2}$	–459.5730806	–459.5753225	–459.5753600	–459.5753744	–459.5753574	–459.5753568
3	$3s^23p^3\ ^2P_{3/2}$	–459.5020317	–459.5042827	–459.5043388	–459.5043395	–459.5043276	–459.5043257
	N_{CSFs}	3	1941	1941	3	3	3

irreducible tensorial form, the CSFs space consists only of 3 CSFs in the CV RCI+RSMBPT computations compared to 1,941 CSFs that are in the ordinary RCI calculations (CV RCI) and in the CV RCI ZF. Such significant CSFs reductions also reduce the matrix and CPU computing time.

4.2. The second test case

In this case, the same test as described above is chosen. We use the program which is designed to determine the contribution of each K' configuration of CV correlations for CSF for which energy needs to be calculated according to the Rayleigh–Schrödinger perturbation theory in an irreducible tensorial form by Eq. (22). The program gives the total contribution of CV correlations with the selected core and virtual orbitals, and calculates the contribution of each K' configuration of the CV correlations for the computed levels. K' configurations are sorted in a descending order according to the effect of CV correlations upon each level. Further, we select K' configurations by the CV correlations effect with the specified fraction of the total CV contribution, and perform RCI computations including them. These fractions are presented in the percentage. The results from the computations when the CV correlations are included using the method described above are marked as CV RCI (RSMBPT), and usual RCI calculations (when all CV correlations are included) are marked as CV RCI and are given in Table 7. There are also energies without CV correlations (marked as MR). In both (CV RCI and CV RCI (RSMBPT)) computations the ZF method is also applied (the MR space is used as the principal part P).

As seen from the results, by including step-by-step the most important K' configurations of CV correlations, the results smoothly converge to the CV RCI computations. In the case when 99.995% of CV correlations are included in the computations, we reproduce the results of usual RCI computations. The convergence by including the most important K' configurations of CV correlations for computed 3 energy levels is displayed in Fig. 9. The trend of inclusion of the most important CV correlations in the ZF case is very similar. From Table 7 it is seen that in the case when 99.995% of CV correlations are included, the CSFs space decreases about 27% compared to the space in CV RCI computations. By using the Rayleigh–Schrödinger perturbation theory

Table 7. The energy levels (in cm^{-1}) and total energies (in a.u.) for 3 energy levels of the $3s^23p^3$ configuration with $J = 3/2$ are given from both computations when CV correlations are included (L1).

No.	State	MR	CV RCI	CV RCI (RSMBPT)					
				95%	99%	99.5%	99.95%	99.995%	99.999999%
				Energy levels (cm^{-1})					
1	$3s^23p^3\ ^4S_{3/2}$	0.00	0.00	0.00	0.00	0.00	0.00	0.00	0.00
2	$3s^23p^3\ ^2D_{3/2}$	23142.25	23141.15	23141.71	23141.27	23141.18	23141.15	23141.15	23141.15
3	$3s^23p^3\ ^2P_{3/2}$	38735.68	38732.59	38734.73	38733.04	38732.78	38732.62	38732.61	38732.61
				Total energy (a.u.)					
1	$3s^23p^3\ ^4S_{3/2}$	−459.6785245	−459.6807614	−459.6806652	−459.6807441	−459.6807518	−459.6807602	−459.6807612	−459.6807613
2	$3s^23p^3\ ^2D_{3/2}$	−459.5730806	−459.5753225	−459.5752238	−459.5753047	−459.5753129	−459.5753214	−459.5753223	−459.5753224
3	$3s^23p^3\ ^2P_{3/2}$	−459.5020317	−459.5042827	−459.5041768	−459.5042634	−459.5042723	−459.5042814	−459.5042824	−459.5042825
				ZF					
				Energy levels (cm^{-1})					
1	$3s^23p^3\ ^4S_{3/2}$	0.00	0.00	0.00	0.00	0.00	0.00	0.00	0.00
2	$3s^23p^3\ ^2D_{3/2}$	23142.25	23136.12	23136.75	23136.28	23136.18	23136.13	23136.12	23136.12
3	$3s^23p^3\ ^2P_{3/2}$	38735.68	38723.48	38725.86	38723.97	38723.69	38723.47	38723.48	38723.48
				Total energy (a.u.)					
1	$3s^23p^3\ ^4S_{3/2}$	−459.6785245	−459.6807760	−459.6806803	−459.6807590	−459.6807667	−459.6807749	−459.6807758	−459.6807760
2	$3s^23p^3\ ^2D_{3/2}$	−459.5730806	−459.5753600	−459.5752615	−459.5753423	−459.5753505	−459.5753590	−459.5753599	−459.5753600
3	$3s^23p^3\ ^2P_{3/2}$	−459.5020317	−459.5043388	−459.5042323	−459.5043196	−459.5043286	−459.5043378	−459.5043387	−459.5043388
	N_{CSFs}	3	1941	678	977	1088	1263	1400	1609

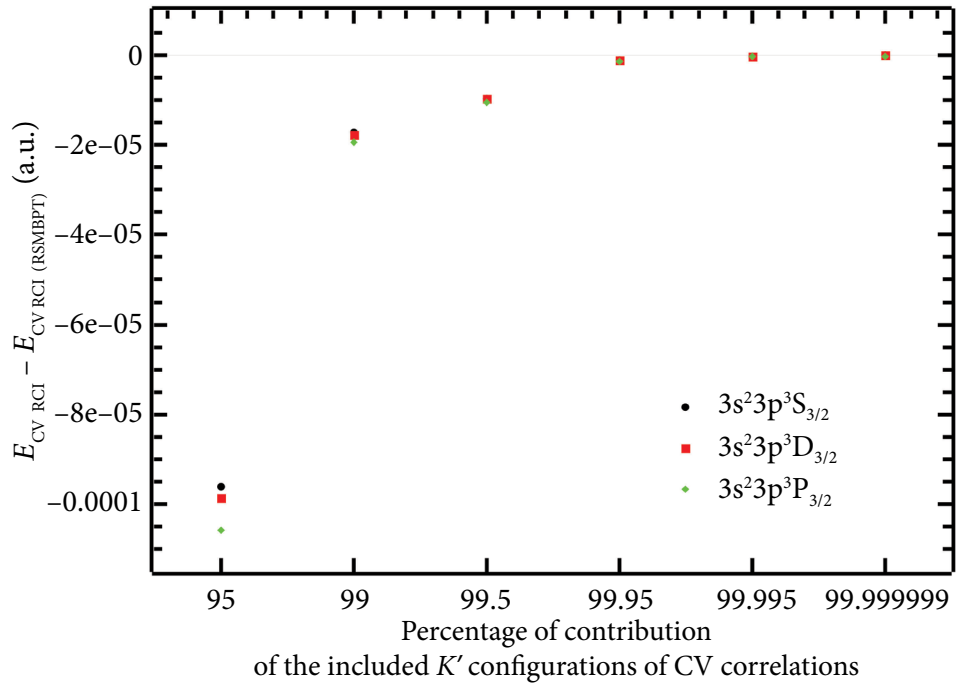

Fig. 9. The convergence by including the most important K' configurations of CV correlations for the computed 3 energy levels of the $3s^23p^3$ configuration with $J = 3/2$.

in an irreducible tensorial form in such a way, we can collect the most important CV correlations, thus the CSFs space is decreased (the matrix and the computing CPU time are reduced).

We will take one more example to present the results of the CV correlations from CV RCI and CV RCI (RSMBPT). We will change the virtual orbitals to the highest ones (9s, 9p_, 9p, 9d_,

Table 8. The energy levels (in cm^{-1}) and total energies (in a.u.) for 3 energy levels of the $3s^23p^3$ configuration with $J = 3/2$ are given from both computations when CV correlations are included (L5).

No.	State	MR	CV RCI	CV RCI (RSMBPT)					
				95%	99%	99.5%	99.95%	99.995%	99.999999%
				Energy levels (cm^{-1})					
1	$3s^23p^3\ ^4S_{3/2}$	0.00	0.00	0.00	0.00	0.00	0.00	0.00	0.00
2	$3s^23p^3\ ^2D_{3/2}$	23142.25	23141.47	23141.84	23141.61	23141.55	23141.48	23141.48	23141.47
3	$3s^23p^3\ ^2P_{3/2}$	38735.68	38710.07	38710.92	38710.05	38710.18	38710.10	38710.07	38710.07
				Total energy (a.u.)					
1	$3s^23p^3\ ^4S_{3/2}$	−459.6785245	−459.6797756	−459.6797214	−459.6797669	−459.6797713	−459.6797752	−459.6797755	−459.6797756
2	$3s^23p^3\ ^2D_{3/2}$	−459.5730806	−459.5743353	−459.5742794	−459.5743259	−459.5743306	−459.5743348	−459.5743352	−459.5743353
3	$3s^23p^3\ ^2P_{3/2}$	−459.5020317	−459.5033995	−459.5033415	−459.5033909	−459.5033947	−459.5033989	−459.5033995	−459.5033995
				ZF					
				Energy levels (cm^{-1})					
1	$3s^23p^3\ ^4S_{3/2}$	0.00	0.00	0.00	0.00	0.00	0.00	0.00	0.00
2	$3s^23p^3\ ^2D_{3/2}$	23142.25	23140.70	23141.08	23140.82	23140.76	23140.71	23140.70	23140.70
3	$3s^23p^3\ ^2P_{3/2}$	38735.68	38708.85	38709.76	38708.84	38708.96	38708.89	38708.86	38708.85
				Total energy (a.u.)					
1	$3s^23p^3\ ^4S_{3/2}$	−459.6785245	−459.6797795	−459.6797259	−459.6797709	−459.6797753	−459.6797791	−459.6797795	−459.6797795
2	$3s^23p^3\ ^2D_{3/2}$	−459.5730806	−459.5743428	−459.5742873	−459.5743336	−459.5743382	−459.5743423	−459.5743427	459.5743428
3	$3s^23p^3\ ^2P_{3/2}$	−459.5020317	−459.5034090	−459.5033512	−459.5034005	−459.5034043	−459.5034084	−459.5034090	−459.5034090
	N_{CSFs}	3	10396	2897	4317	4648	5136	5509	6182

9d, 8f_, 8f, 8g_, 8g, 8h_, 8h, 8i_, 8i, set of these virtual orbitals will be marked as L5) in the test case described above. The results are presented in Table 8. It is seen that the results from CV RCI (RSMBPT) smoothly converge to the CV RCI computations. In the case when 99.95% of CV correlations are included in the computations, the results are very close to the CV RCI computations, and in the case of 99.995% the results of usual RCI computations are reproduced. When 99.995% of CV correlations are included, the CSFs space decreases about 47% compared to the space in CV RCI computations. Comparing the results from this test with those of the previous test (with smaller virtual orbitals) it is seen that the contribution of CV correlations decreases (as it is known). However, using the Rayleigh–Schrödinger perturbation theory in an irreducible tensorial form in such a way, we can calculate and estimate the contribution of each K' of the CV correlations with the preferred core and virtual orbitals. That allows us to select the most important CV correlations and perform the RCI computations in the space of CSFs that is significantly reduced.

5. Summary and conclusions

The Rayleigh–Schrödinger perturbation theory in a nonrelativistic approach [9, 10] was extended to a relativistic approach in such a way that the Feynman diagrams corresponding to the core–valence correlation are presented in an irreducible tensorial form in the *jj*-coupling. This allows us to use the spin-angular library [5, 11] without any modifications and to make the easiest implementation of this theory in the Grasp2018 package [8] in general. Two proposed computational methods (CV RCI+RSMBPT and CV RCI (RSMBPT)), which combine the RCI method and the stationary second-order Rayleigh–Schrödinger many-body perturbation theory in an irreducible tensorial form, allows us to include the core–valence correlations for atoms or ions with any number of valence electrons in a simplified way instead of the large RCI computations. Rayleigh–Schrödinger perturbation theory in an irreducible tensorial form has several advantages over the Brillouin–Wigner perturbation theory implemented in the Grasp code [12, 8]: firstly, the space of CSFs is significantly reduced, which leads to a smaller matrix and its simpler diagonalization. So the computational resources needed for computations and the computing CPU time are also reduced. In addition, this computational method allows us to include the CV correlations from the deeper core.

References

[1] C. Froese Fischer, *The Hartree-Fock Method for Atoms* (Wiley, New York, 1997).

[2] I.P. Grant, *Relativistic Quantum Theory of Atoms and Molecules* (Springer, New York, 2007).

[3] I. Lindgren and J. Morrison, *Atomic Many-body Theory* (Springer-Verlag Berlin Heidelberg, New York, 1982).

[4] G. Gaigalas and Z. Rudzikas, On the secondly quantized theory of the many-electron atom, J. Phys. B **29**(15), 3303 (1996), https://doi.org/10.1088/0953-4075/29/15/007

[5] G. Gaigalas, Z. Rudzikas, and C. Froese Fischer, An efficient approach for spin-angular integrations in atomic structure calculations, J. Phys. B **30**(17), 3747 (1997), https://doi.org/10.1088/0953-4075/30/17/006

[6] P. Bogdanovich, G. Gaigalas, A. Momkauskaitė, and Z. Rudzikas, Accounting for admixed configurations in the second order of perturbation theory for complex atoms, Phys. Scr. **56**, 230–239 (1997), https://doi.org/10.1088/0031-8949/56/3/002

[7] V.A. Dzuba and V.V. Flambaum, Core-valence correlations for atoms with open shells, Phys. Rev. A **75**, 052504 (2007), https://doi.org/10.1103/PhysRevA.75.052504

[8] C. Froese Fischer, G. Gaigalas, P. Jönsson, and J. Bieroń, Grasp2018 – A Fortran 95 version of the General Relativistic Atomic Structure package, Comput. Phys. Commun. **237**, 184–187 (2019), https://doi.org/10.1016/j.cpc.2018.10.032

[9] G. Merkelis, G. Gaigalas, J. Kaniauskas, and Z. Rudzikas, Application of the graphical method of the angular momentum theory to the study of the stationary perturbation series, Izvest. Acad. Nauk SSSR, Phys. Coll. **50**, 1403–1410 (1986) [in Russian].

[10] G. Gaigalas, *Irreducible Tensorial Form of the Stationary Perturbation Theory for Atoms and*

Ions with Open Shells, PhD Thesis (Institute of Physics, Vilnius, 1989) [in Russian].

[11] G. Gaigalas, A program library for computing pure spin-angular coefficients for one- and two-particle operators in relativistic atomic theory, Atoms **10**(4), 129 (2022), https://doi.org/10.3390/atoms10040129

[12] P. Jönsson, G. Gaigalas, J. Bieroń, C. Froese Fischer, and I.P. Grant, New version: GRASP2K relativistic atomic structure package, Comput. Phys. Commun. **184**(9), 2197–2203 (2013), https://doi.org/10.1016/j.cpc.2013.02.016

[13] C. Froese Fischer, M. Godefroid, T. Brage, P. Jönsson, and G. Gaigalas, Advanced multi-configuration methods for complex atoms: I. Energies and wave functions, J. Phys. B **49**(18), 182004 (2016), https://doi.org/10.1088/0953-4075/49/18/182004

[14] P. Jönsson, M. Godefroid, G. Gaigalas, J. Ekman, J. Grumer, W. Li, J. Li, T. Brage, I.P. Grant, J. Bieroń, and C. Froese Fischer, An introduction to relativistic theory as implemented in GRASP, Atoms **11**(1), 7 (2023), https://doi.org/10.3390/atoms11010007

[15] K.G. Dyall, I.P. Grant, C.T. Johnson, F.A. Parpia, and E.P. Plummer, GRASP: A general-purpose relativistic atomic structure program, Comput. Phys. Commun. **55**(3). 425–456 (1989), https://doi.org/10.1016/0010-4655(89)90136-7

[16] D. Kato, X.M. Tong, H. Watanabe, T. Fukami, T. Kinugawa, C. Yamada, S. Ohtani, and T. Watanabe, Fine-structure in $3d^4$ states of highly charged Ti-like ions, J. Chin. Chem. Soc. **48**(3), 525–529 (2001).

[17] A.P. Yutsis, I.B. Levinson, and V.V. Vanagas, *Mathematical Apparatus of the Theory of Angular Momentum* (Israel Program for Scientific Translations Ltd, 1962).

[18] A.P. Jucys and A.A. Bandzaitis, *Theory of Angular Momentum in Quantum Mechanics* (Mokslas, Vilnius, 1977) [in Russian].

[19] U. Fano and G. Racah, *Irreducible Tensorial Sets* (Academic Press, 1959).

[20] B.R. Judd, *Second Quantization and Atomic Spectroscopy* (The Johns Hopkins Press, Baltimore, MD, 1967).

[21] Z. Rudzikas and J. Kaniauskas, *Quasispin and Isospin in the Theory of Atom* (Mokslas, Vilnius, 1984) [in Russian].

[22] G. Gaigalas, J.G. Kaniauskas, and Z. Rudzikas, Diagrammatic technique of the angular momentum theory and second quantization, Liet. Fiz. Rink. (Sov. Phys. Coll.) **25**, 3–13 (1985) [in Russian].

[23] Z. Rudzikas, *Theoretical Atomic Spectroscopy* (Cambridge University Press, Cambridge, 1997).

[24] G. Gaigalas, S. Fritzsche, and Z. Rudzikas, Reduced coefficients of fractional parentage and matrix elements of the tensor $W^{(k_q k_j)}$ in *jj*-coupling, At. Data Nucl. Data Tables **76**(2), 235–269 (2000), https://doi.org/10.1006/adnd.2000.0844

[25] G. Merkelis, G. Gaigalas, and Z. Rudzikas, Irreducible tensorial form of the effective Hamiltonian of an atom and the diagrammatic representation in the first two orders of the stationary perturbation theory, Liet. Fiz. Rink. (Sov. Phys. Coll.) **25**, 14–31 (1985) [in Russian].

[26] P. Jönsson, G. Gaigalas, Ch. F. Fischer, J. Bieroń, I.P. Grant, T. Brage, J. Ekman, M. Godefroid, J. Grumer, J. Li, and W. Li, GRASP manual for users, Atoms, **11**, 68 (2023), https://doi.org/10.3390/atoms11040068

[27] S. Gustafsson, P. Jönsson, C. Froese Fischer, and I.P. Grant, Combining multiconfiguration and perturbation methods: Perturbative estimates of core-core electron correlation contributions to excitation energies in Mg-like iron, Atoms **5**(1), 3 (2017), https://doi.org/10.3390/atoms5010003

[28] P. Jönsson, G. Gaigalas, P. Rynkun, L. Radžiūtė, J. Ekman, S. Gustafsson, H. Hartman, K. Wang, M. Godefroid, C. Froese Fischer, I. Grant, T. Brage, and G. Del Zanna, Multiconfiguration Dirac-Hartree-Fock calculations with spectroscopic accuracy: Applications to astrophysics, Atoms **5**, 16 (2017), https://doi.org/10.3390/atoms5020016

[29] P. Bogdanovich, G. Gaigalas, and A. Momkauskaitė, Accounting for correlation corrections to interconfigurational matrix elements, Lith. J. Phys. **38**(5), 443–451 (1998) [in Russian].

[30] R. Karazija, *Introduction to the Theory of X-ray and Electronic Spectra of Free Atoms* (Plenum Press, New York, 1996).

[31] G. Gaigalas, P. Rynkun, L. Radžiūtė, D. Kato, M. Tanaka, and P. Jönsson, Energy level structure and transition data of Er^{2+}, Astrophys. J. Suppl. Ser. **248**(1), 13 (2020), https://doi.org/10.3847/1538-4365/ab881a

[32] G. Gaigalas, P. Rynkun, L. Radžiūtė, P. Jönsson, and K. Wang, Energy and transition data computations for P-like ions: As, Kr, Sr, Zr, Mo, and W, At. Data Nucl. Data Tables **141**, 101428 (2021), https://doi.org/10.1016/j.adt.2021.101428

[33] Y.T. Li, K. Wang, R. Si, M. Godefroid, G. Gaigalas, Ch.Y. Chen, and P. Jönsson, Reducing the computational load – atomic multiconfiguration calculations based on configuration state function generators, Comput. Phys. Commun. **283**, 108562 (2023), https://doi.org/10.1016/j.cpc.2022.108562

[34] P. Bogdanovich and R. Kisielius, Theoretical energy level spectra and transition data for $4p^64d$, $4p^64f$ and $4p^54d^2$ configurations of W^{37+} ion, At. Data Nucl. Data Tables **98**(4), 557–565 (2012), https://doi.org/10.1016/j.adt.2011.11.004

[35] P. Bogdanovich and R. Kisielius, Theoretical energy level spectra and transition data for $4p^64d^2$, $4p^64d4f$, and $4p^54d^3$ configurations of W^{36+}, At. Data Nucl. Data Tables **99**(5), 580–594 (2013), https://doi.org/10.1016/j.adt.2012.11.001

[36] R. Karpuškienė and R. Kisielius, Theoretical level energies and transition data for $4p^64d^8$, $4p^54d^9$ and $4p^64d^74f$ configurations of W^{30+} ion, At. Data Nucl. Data Tables **143**, 101478 (2022), https://doi.org/10.1016/j.adt.2021.101478

[37] R. Kisielius, V.P. Kulkarni, G.J. Ferland, P. Bogdanovich, D. Som, and M.L. Lykins, Atomic data for Zn II: Improving spectral diagnostics of chemical evolution in high-redshift galaxies, Astrophys. J. **804**(1), 76 (2015), https://doi.org/10.1088/0004-637X/804/1/76

[38] P. Bogdanovich, Modern methods of multi-configuration studies of many-electron highly charged ions, Nucl. Instrum. Methods Phys. Res. B **235**(1–4), 92–99 (2005), https://doi.org/10.1016/j.nimb.2005.03.152

[39] P. Bogdanovich, R. Karpuškienė, and Z. Rudzikas, Calculation of electronic transitions in S IX, Phys. Scr. **T80B**, 474–475 (1999), https://doi.org/10.1238/Physica.Topical.080a00474

[40] R. Karpuškienė, P. Bogdanovich, and R. Kisielius, Significance of $M2$ and $E3$ transitions for $4p^54d^{N+1}$- and $4p^64d^{N-1}4f$-configuration metastable-level lifetimes, Phys. Rev. A **88**, 022519 (2013), https://doi.org/10.1103/PhysRevA.88.022519

[41] K.M. Aggarwal, P. Bogdanovich, F.P. Keenan, and R. Kisielius, Energy levels and radiative rates for Cr-like Cu VI and Zn VII, At. Data Nucl. Data Tables **111–112**, 280–345 (2016), https://doi.org/10.1016/j.adt.2016.03.001

[42] R. Karpuškienė, P. Bogdanovich, and A. Udris, *Ab initio* oscillator strengths and radiative lifetimes for Ca IX, J. Phys. B **37**(10), 2067 (2004), https://doi.org/10.1088/0953-4075/37/10/006

[43] P. Bogdanovich, R. Karpuškienė, and I. Martinson, Theoretical calculation of transition probabilities and lifetimes of levels of the $4d^95p$ configuration of Cd III, Opt. Spectrosc. **90**(1), 4–7 (2001), https://doi.org/10.1134/1.1343537

[44] P. Rynkun, G. Gaigalas, and P. Jönsson, Theoretical investigation of energy levels and transition data for S II, Cl III, Ar IV, Astron. Astrophys. **623**, A155 (2019), https://doi.org/10.1051/0004-6361/201834931

ANTROSIOS EILĖS RELĖJAUS IR ŠRĖDINGERIO TRIKDYMŲ TEORIJA GRASP2018 PROGRAMINIAM PAKETUI: KAMIENO IR VALENTINĖS KORELIACIJOS*

G. Gaigalas, P. Rynkun, L. Kitovienė

Vilniaus universiteto Teorinės fizikos ir astronomijos institutas, Vilnius, Lietuva

Santrauka

GRASP programinis paketas [GRASP2018, C. Froese Fischer, G. Gaigalas, P. Jönsson, J. Bieroń, Comput. Phys. Commun. (2019), DOI: 10.1016/j.cpc.2018.10.032] grindžiamas daugiakonfigūraciniu Dirako, Hartrio ir Foko bei reliatyvistiniu konfigūracijų superpozicijos (RCI) metodais, skirtais atomų ir jonų energijos struktūros skaičiavimams. Programoje naudojama atominė būsenos funkcija sudaryta iš konfigūracinių būsenų funkcijų rinkinio. RCI metode valentinės-valentinės, kamieno-valentinės ir kamieno-kamieno koreliacijos yra tiesiogiai įtrauktos į atomo būsenos funkciją per konfigūracinių būsenų funkcijas. Šiame darbe pateiktas naujas efektyvesnis kamieno-valentinių koreliacijų įskaitymo būdas. Jis sukurtas remiantis RCI ir stacionarios daugiadalelės trikdžių teorijos neredukuotinėje tenzorinėje formoje kombinacija. Tai leidžia įskaityti kamieno-valentines koreliacijas, naudojant trikdžių teoriją bet kokiam atomui ir jonui su bet kokiu valentinių elektronų skaičiumi. Šis naujai sukurtas metodas, kurį galima naudoti dviem būdais, leidžia gerokai sumažinti konfigūracinių būsenų funkcijų erdvę sudėtingiems atomams ir jonams, kas daug lengviau leidžia išplėsti GRASP programinio paketo galimybes. Darbe pademonstruota, kaip šis metodas veikia apskaičiuojant Cl III jono energijos struktūrą.

* Skiriama šiuolaikinės teorinės fizikos Lietuvoje pradininko, „Lietuvos fizikos rinkinio“ iniciatoriaus akad. **Adolfo Jucio** (1904–1974) gimimo ir mirties sukaktims paminėti.